



Comparative study of the reliability of MPPT algorithms for the crystalline silicon photovoltaic modules in variable weather conditions

Abraham Dandoussou^{a,*}, Martin Kamta^b, Laurent Bitjoka^b,
Patrice Wira^c, Alexis Kuitché^b

^a Department of Electrical and Power Engineering, Higher Technical Teachers' Training College (HTTTC), University of Buea, Kumba, Cameroon

^b Laboratory of energy, signal, image and automation (LESIA), National School of Agro-Industrial Sciences, University of Ngaoundere, P. O. Box 455 Ngaoundere, Cameroon

^c Laboratory MIPS, University of Haute Alsace, 61 Road Albert Camus, 68093 Mulhouse Cedex, France

Received 21 November 2015; received in revised form 23 July 2016; accepted 15 August 2016

Abstract

The crystalline silicon photovoltaic modules are widely used as power supply sources in the tropical areas where the weather conditions change abruptly. Fortunately, many MPPT algorithms are implemented to improve their performance. In the other hand, it is well known that these power supply sources are nonlinear dipoles and so, their intrinsic parameters may vary with the irradiance and the temperature. In this paper, the MPPT algorithms widely used, i.e. Perturb and Observe (P&O), Incremental Conductance (INC), Hill-Climbing (HC), are implemented using Matlab[®]/Simulink[®] model of a crystalline silicon photovoltaic module whose intrinsic parameters were extracted by fitting the I(V) characteristic to experimental points. Comparing the simulation results, it is obvious that the variable step size INC algorithm has the best reliability than both HC and P&O algorithms for the near to real Simulink[®] model of photovoltaic modules. With a 60 Wp photovoltaic module, the daily maximum power reaches 50.76 W against 34.40 W when the photovoltaic parameters are fixed. Meanwhile, the daily average energy is 263 Wh/day against 195 Wh/day.

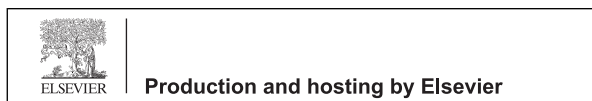
© 2016 Electronics Research Institute (ERI). Production and hosting by Elsevier B.V. This is an open access article under the CC BY-NC-ND license (<http://creativecommons.org/licenses/by-nc-nd/4.0/>).

Keywords: Crystalline silicon photovoltaic module; Fittings; MPPT algorithms; Modelling; Simulation

* Corresponding author.

E-mail addresses: abraham.dandoussou@ubuea.cm (A. Dandoussou), martin.kamta@yahoo.fr (M. Kamta), lbitjoka@univ-ndere.cm (L. Bitjoka), patrice.wira@uha.fr (P. Wira), kuitche_a@yahoo.fr (A. Kuitché).

Peer review under the responsibility of Electronics Research Institute (ERI).



<http://dx.doi.org/10.1016/j.jesit.2016.08.008>

2314-7172/© 2016 Electronics Research Institute (ERI). Production and hosting by Elsevier B.V. This is an open access article under the CC BY-NC-ND license (<http://creativecommons.org/licenses/by-nc-nd/4.0/>).

Please cite this article in press as: Dandoussou, A., et al., Comparative study of the reliability of MPPT algorithms for the crystalline silicon photovoltaic modules in variable weather conditions. J. Electr. Syst. Inform. Technol. (2016), <http://dx.doi.org/10.1016/j.jesit.2016.08.008>

1. Introduction

It is well known that the operating point of a photovoltaic power supply source moves away from its maximum power point when the irradiance changes (Kumar, 2013; Abdulkadir et al., 2013; Durusu et al., 2014a; de Brito et al., 2013). To solve this problem, various MPPT algorithms have been implemented (Abdulkadir et al., 2013; Durusu et al., 2014a; de Brito et al., 2013; Rathod et al., 2014). Among these MPPT algorithms, some already have industrial applications because of their ease of implementation, i.e. Perturb and Observe (P&O), Hill Climbing (HC) and Incremental Conductance (INC) algorithms (Durusu et al., 2014a; de Brito et al., 2013; Rathod et al., 2014).

The function of these algorithms is to transfer the maximum power from the photovoltaic power supply source to the DC load. This is possible by inserting a DC–DC converter between the photovoltaic power supply source and the DC load. Such algorithms are implemented on an electronic control circuit of the DC–DC boost or buck converter. Thus, the transfer of the maximum power to the load is achieved when the output impedance of the DC–DC converter is comparable with the DC load. To do this, the converter output impedance may be modulated by the duty cycle of the control signal according to the values of the irradiance.

In the literature, most MPPT algorithms do not take into consideration the variations of the intrinsic parameters of the photovoltaic power supply source such as the series resistance and the reverse saturation current (de Brito et al., 2013; Rathod et al., 2014). However, it has been shown that these intrinsic parameters depend closely on weather conditions (Dandoussou et al., 2015).

The main objective of this paper is to compare the reliability of MPPT algorithms that do not take into consideration changes in the series resistance of crystalline silicon photovoltaic modules with those that take them into consideration under the variable weather conditions. In fact, as mentioned above, MPPT techniques are generally implemented under laboratory conditions with weather conditions (irradiance and temperature) that are produced and controlled by laboratory equipment. These former works did not consider the variations of photovoltaic parameters when the PV module is submitted under normal operating conditions (NOC).

2. MPPT algorithms

2.1. Perturb and Observe algorithm

The P&O algorithm is the only one that is implemented and sold in the markets. Its principle is to perturb the output voltage or current of a PV module and observe the output power at the same time. In fact, this technique searches for the maximum power point (MPP) while checking the sign of the differential coefficient of the power with respect to the voltage (dP_{pv}/dV_{pv}) in the P–V characteristics. Unfortunately, the steady state is always unstable (Alsadi and Alsayid, 2012; Saxena and Gupta, 2014).

According to the P–V characteristic of a PV module and its derivative (dP_{pv}/dV_{pv}) as shown in Fig. 1, three cases can be distinguished:

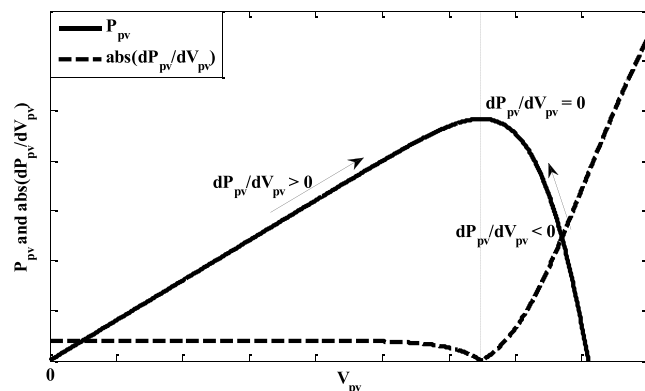


Fig. 1. P–V characteristic of a PV module.

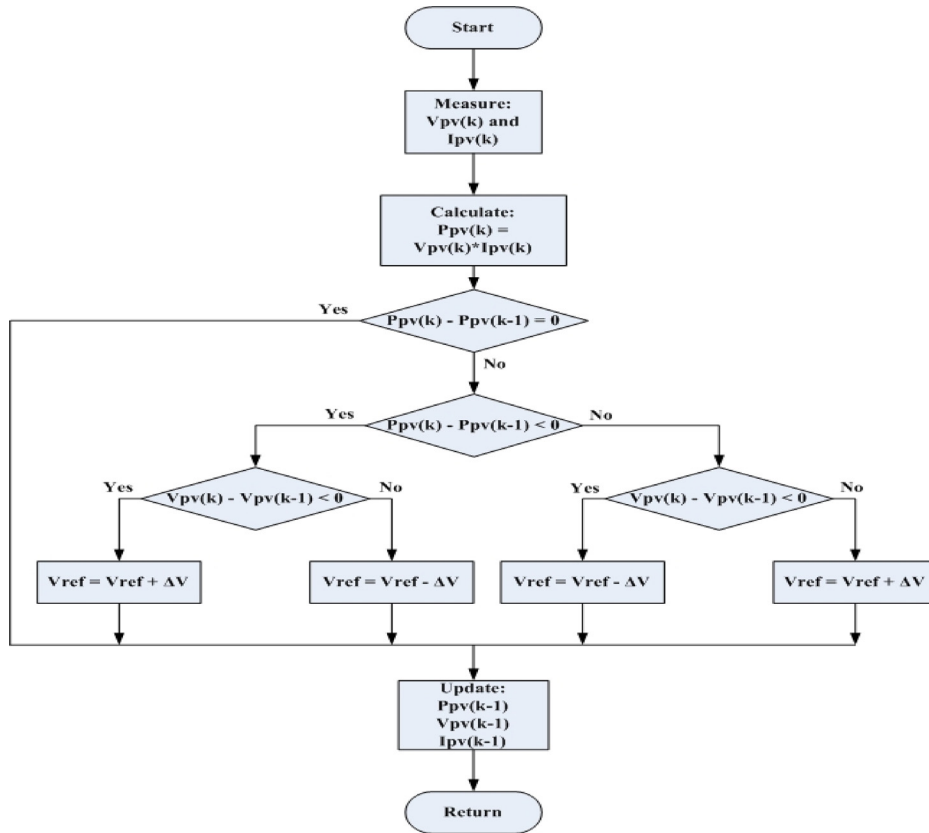


Fig. 2. Flowchart of the P&O algorithm.

- When $\frac{dP_{pv}}{dV_{pv}} = 0$, the operating point coincided with the MPP.
- When $\frac{dP_{pv}}{dV_{pv}} > 0$, the operating point is located on the left side of the MPP. So, the voltage shall be increased until the MPP is reached.
- When $\frac{dP_{pv}}{dV_{pv}} < 0$, the operating point is located on the right side of the MPP. So, the voltage shall be decreased until the MPP is reached.

In this study, Matlab[®] environment is used to simulate the results. In fact, nowadays, Matlab[®] is the most used software in computer aided design and research work. Fig. 2 shows the flowchart of this algorithm and Fig. 3 shows its Matlab[®]/Simulink[®] flowchart. The simulation results will be shown in Section 4.

2.2. Hill Climbing algorithm

This algorithm is using the sign of the derivative of the output power with respect to the voltage or the current (Alsadi and Alsayid, 2012; Saxena and Gupta, 2014).

- When $\frac{dP_{pv}}{dV_{pv}} > 0$, the duty cycle D should be increased by a step ΔD .
- When $\frac{dP_{pv}}{dV_{pv}} < 0$, the duty cycle D should be decreased by a step ΔD .

Fig. 4 shows the flowchart of the algorithm and Fig. 5 shows its Matlab[®]/Simulink[®] flowchart. The simulation results will be shown in Section 4.

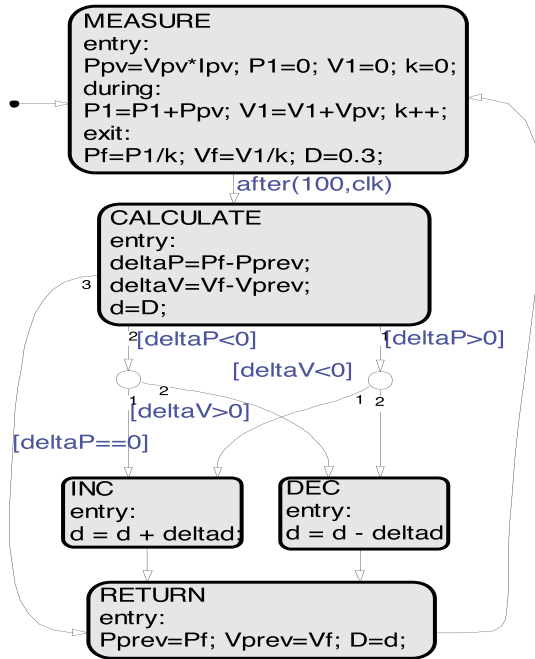


Fig. 3. The Matlab®/Simulink® flowchart of the P&O algorithm.

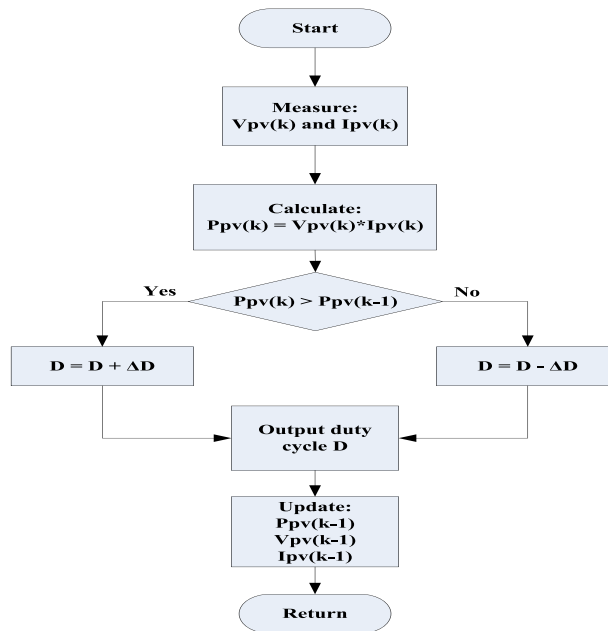


Fig. 4. Flowchart of the Hill Climbing algorithm.

2.3. Incremental Conductance algorithm

This method is also based on the derivative of the output power with respect to the voltage. It reduces the oscillations which have been observed in the P&O method. In fact, it searches for the MPP while checking the sign of the incremental conductance (dI_{pv}/dV_{pv}). Unfortunately, it is difficult to find out the MPP in lower irradiation.

$$dP_{pv}/dV_{pv} = d(V_{pv}I_{pv})/dV_{pv} = I_{pv} + V_{pv}dI_{pv}/dV_{pv} \tag{1}$$

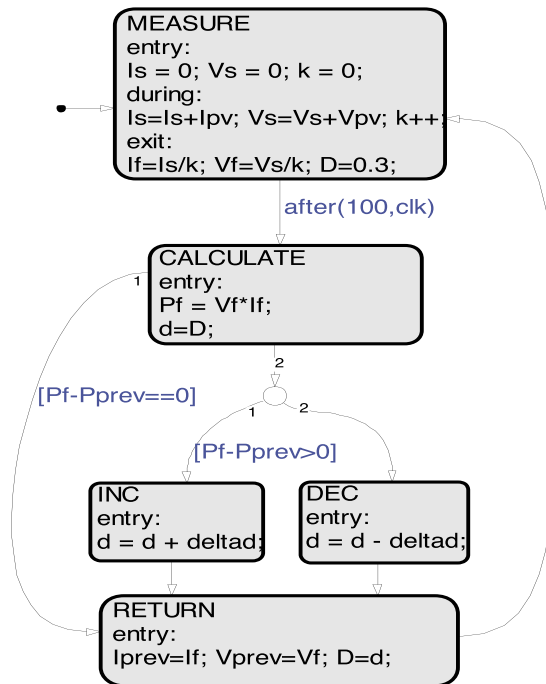


Fig. 5. Matlab®/Simulink® Stateflow chart of the Hill Climbing algorithm.

- When $\frac{dI_{pv}}{dV_{pv}} = -I_{pv}/V_{pv}$, the operating point coincides with the MPP.
- When $\frac{dI_{pv}}{dV_{pv}} > -I_{pv}/V_{pv}$, the operating point is on the left side of the MPP. The duty cycle D shall be decreased by a step ΔD .
- When $\frac{dI_{pv}}{dV_{pv}} < -I_{pv}/V_{pv}$, the operating point is on the right side of the MPP. The duty cycle D shall be increased by a step ΔD .

For a constant step INC, the system will oscillate around the MPP for a high step size ΔD . Meanwhile, it will be stable around the MPP for a small step size ΔD even though it becomes slow (Christopher and Ramesh, 2016; Durusu et al., 2014b; Lokanadham and Vijaya Bhaskar, 2012; Saravana Selvan, 2013; Tey and Mekhilef, 2014). In order to solve this problem, a variable step size INC algorithm has been developed (Cho and Hong, 2013; Liu et al., 2008). The corresponding step size is given by:

$$\Delta D = N \left| \frac{P_{pv}(k) - P_{pv}(k-1)}{V_{pv}(k) - V_{pv}(k-1)} \right| \quad (2)$$

where the coefficient N is a scaling factor. Its value can be obtained by solving Eq. (3) with ΔD_{max} the maximum step size in the previous sampling period.

$$N < \Delta D_{max} / \left| \frac{dP_{pv}}{dV_{pv}} \right|_{fixed \ step} = \Delta D_{max} \quad (3)$$

Another variable step size has been defined as shown in Eq. (4) where the coefficient NP is the scaling factor and ΔP is the variation of the output power (Liu et al., 2008).

$$\Delta D = NP \left| 1 - \frac{1}{1 + \exp(-a(\Delta P - c))} \right| \quad (4)$$

Fig. 6 shows the flowchart of the variable step Incremental Conductance algorithm and Fig. 7 shows its Matlab®/Simulink® flowchart. The simulation results will be shown in Section 4.

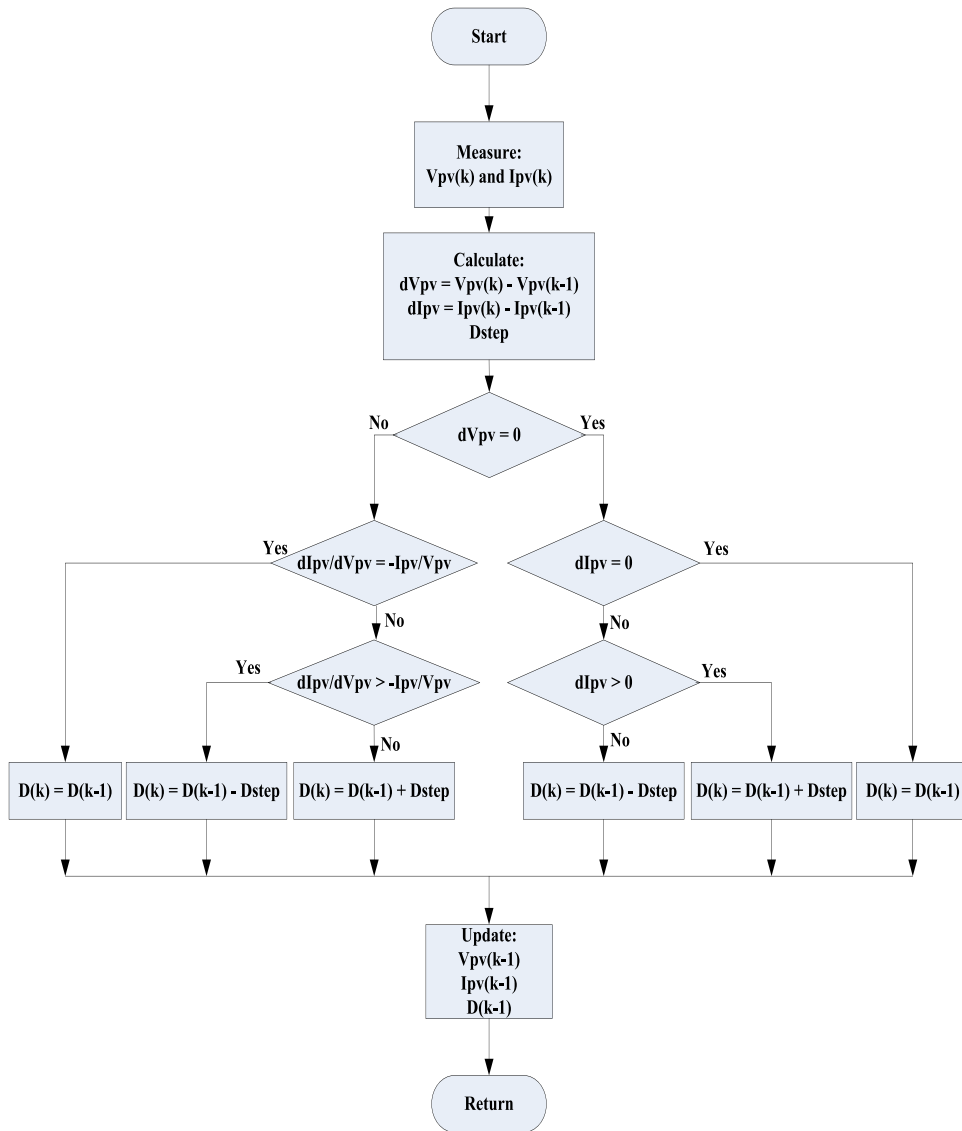


Fig. 6. Flowchart of the variable step Incremental Conductance algorithm.

3. Simulink® model of the photovoltaic system

The Simulink® model of the PV system is shown in Fig. 8, with the following blocs:

- A bloc diagram of the monocrystalline PV module with the manufacturer’s specifications given in Table 1.
- A bloc diagram of a boost DC–DC converter with the parameters calculated and given in Table 2.
- An MPPT bloc with as inputs: the PV module voltage V_{pv} and current I_{pv} , and the step size dD defined only for the P&O, INC and HC algorithms. For the variable step INC, input dD is not defined because the step is calculated in the MPPT bloc.
- A constant resistive load of 7.5Ω .

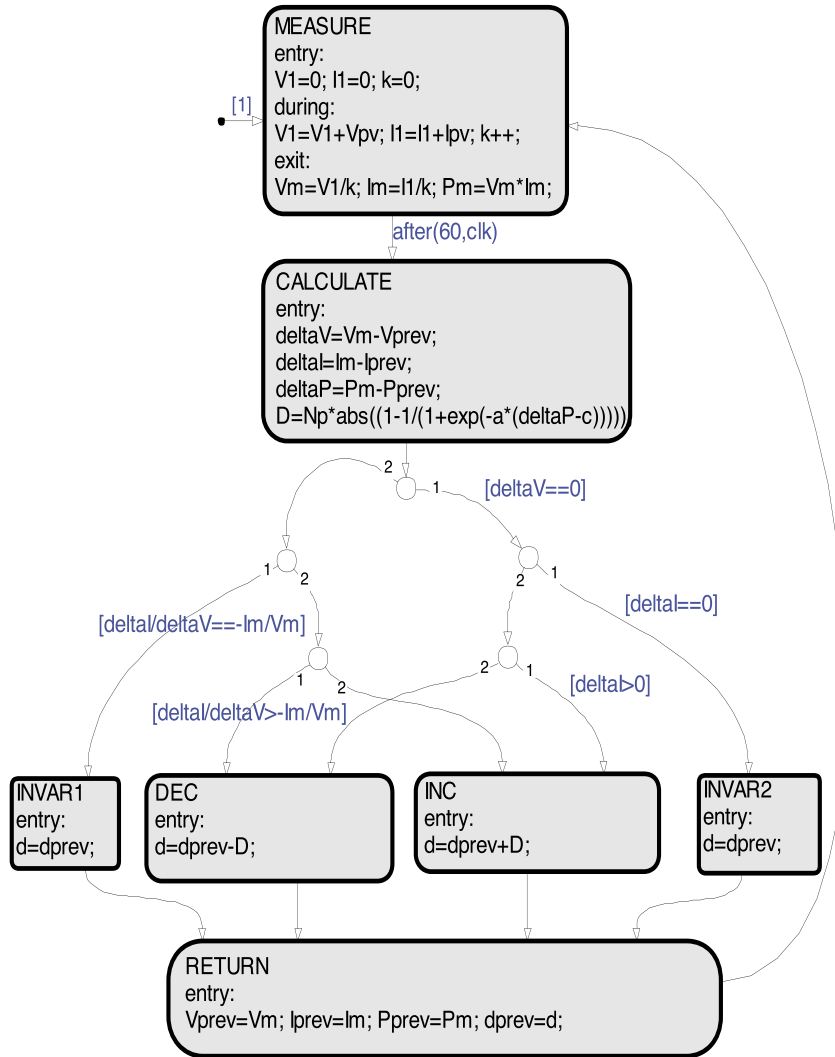


Fig. 7. Matlab®/Simulink® Stateflow chart of the Incremental Conductance algorithm.

Table 1
 Manufacturer’s specifications of the PV module.

Band gap energy of silicon at 300 K	1.12 eV
Short-circuit current at STC	4.01 A
Open circuit voltage at STC	21.6 V
Current at MPP	3.47 A
Voltage at MPP	17.3 V
Maximum power at STC	60 Wp
Number of series-connected cells	36

Table 2
 Parameters of the boost DC–DC converter.

Switching frequency	20 kHz
Inductance value	935 μH
Capacitance value	2.67 μF

Please cite this article in press as: Dandoussou, A., et al., Comparative study of the reliability of MPPT algorithms for the crystalline silicon photovoltaic modules in variable weather conditions. J. Electr. Syst. Inform. Technol. (2016), <http://dx.doi.org/10.1016/j.jesit.2016.08.008>

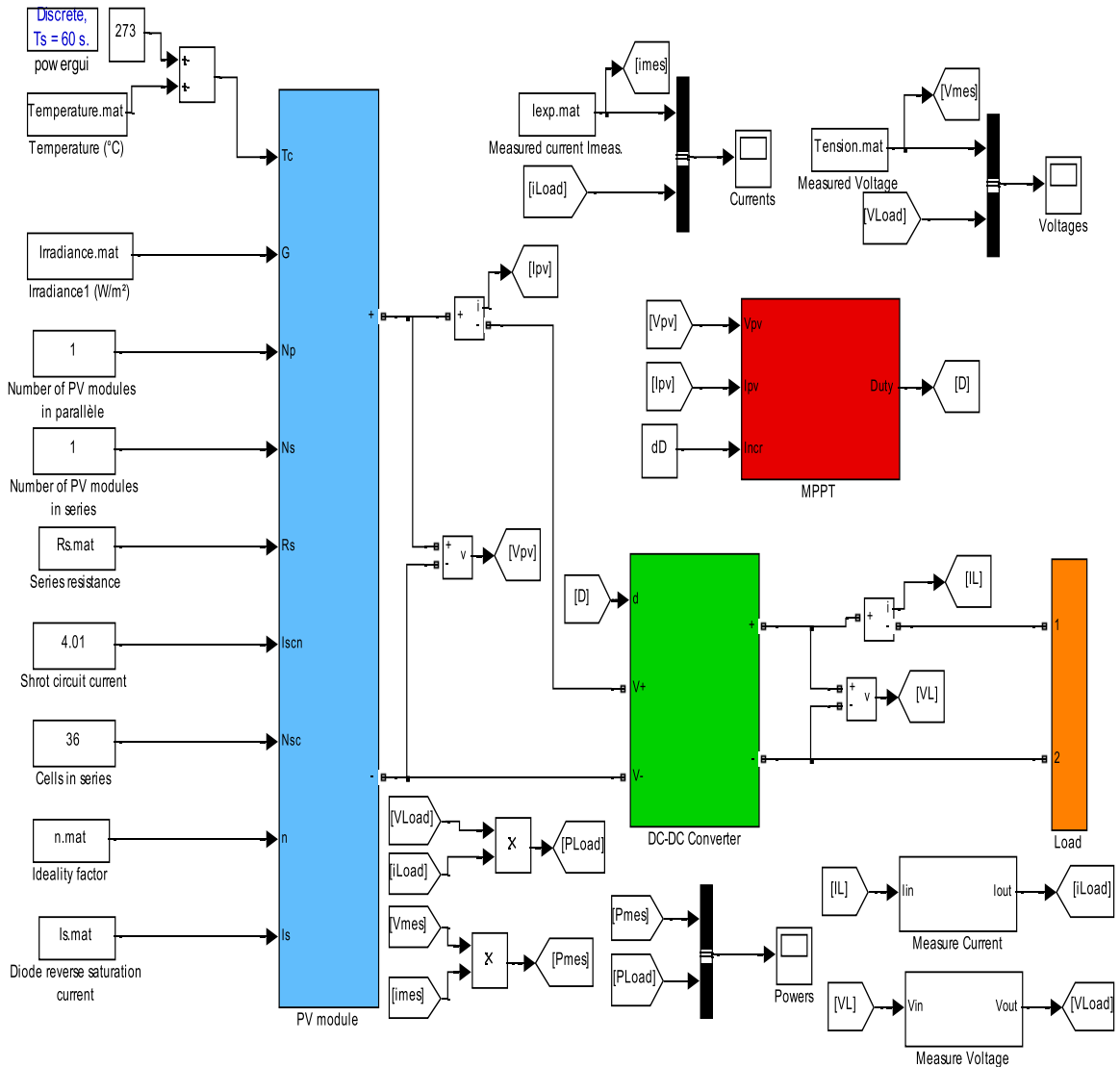


Fig. 8. Simulink® model of the implemented photovoltaic system.

The input variables of the bloc diagram of the PV module are: the irradiance, the temperature and the intrinsic parameters of the PV module (i.e. the diode ideality factor n , the reverse saturation current I_s and the series resistance R_s).

Fig. 9 shows the experimental curves of the irradiance and the temperature recorded during a sunny day from 9:30 A.M. to 02:30 P.M. at local time. Obviously, both the irradiance and the temperature do not have the same profile during the day.

The photovoltaic parameters of the PV module have been determined in a previous work by adjusting the I–V function to the experimental data (Dandoussou et al., 2015). Fig. 10 shows the curves of the intrinsic parameters obtained by fittings. Obviously, the diode ideality factor (n) is almost constant, while the variations of the reverse saturation current (I_s) and the series resistance (R_s) are equivalent to those of the cell temperature and the irradiance respectively.

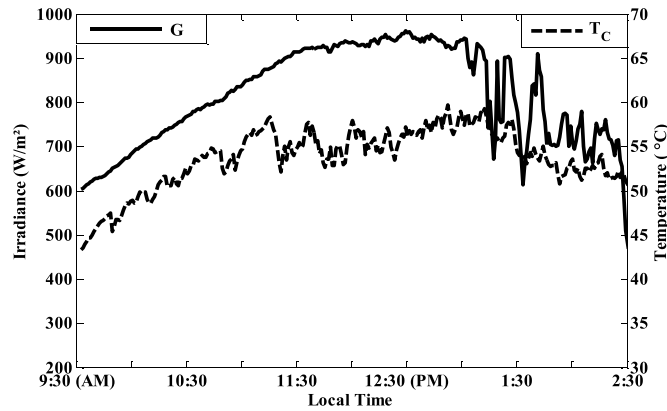


Fig. 9. Curves of the irradiance and the cell temperature recorded during the day of January 23, 2013, at the latitude of 7.3°N and the longitude of 13.3°E.

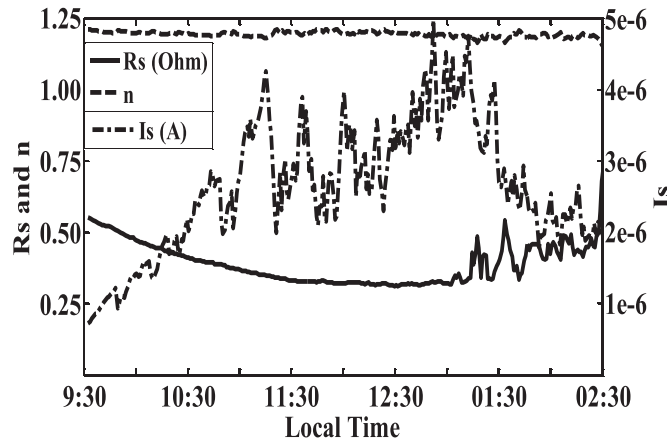


Fig. 10. Curves of the intrinsic parameters of a PV module determined by fittings (Dandoussou et al., 2015).

4. Results and discussion

Firstly, the simulations have been carried out with the constant values of the intrinsic solar cell parameters ($R_s = 2.1 \Omega$ and $n = 1.2$) and secondly, with the intrinsic solar cell parameters depending on the weather conditions as shown in Fig. 10. The step size ΔD has been fixed to 0.01 for the P&O, HC and fixed step INC algorithms.

Fig. 11 shows the simulation and the experimental curves of the output power of the PV module using the P&O algorithm. The simulation curve (dash-dot line) for the intrinsic solar cell parameters depending on weather conditions is higher than the simulation curve (dash line) for the constant intrinsic solar cell parameters. In addition, its profile is almost the same like the profile of the experimental curve measured without an MPPT module (solid line).

Fig. 12 shows the simulation and the experimental curves of the output power of the PV module using the Hill Climbing algorithm. The simulation curve (dash-dot line) for the intrinsic solar cell parameters depending on weather conditions is higher than the simulation curve (dash line) for the constant intrinsic solar cell parameters. In addition, its profile is almost the same like the profile of the experimental curve measured without an MPPT module (solid line).

Figs. 13 and 14 show the simulation and the experimental curves of the output power of the PV module using the Incremental Conductance algorithm, with a constant step size and with a variable step size respectively. For the variable step INC, the different parameters for calculating the step are set as follow: $N_p = 0.0002$, $a = 0.05$ and $c = 150$ (Liu et al., 2008). In both cases, the simulation curve (dash-dot line) for the intrinsic solar cell parameters depending on weather conditions is higher than the simulation curve (dash line) for the constant intrinsic solar cell parameters. In

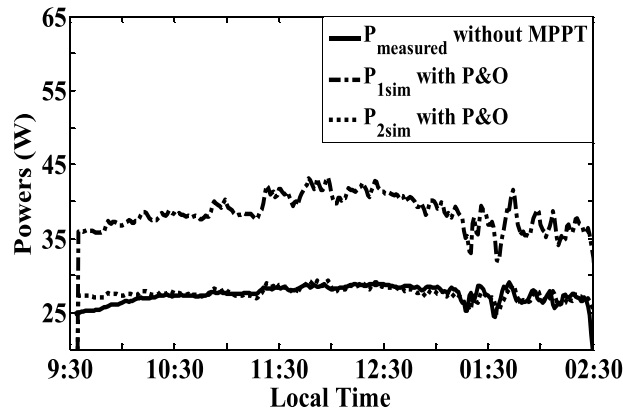


Fig. 11. Curves of output powers of the PV module.

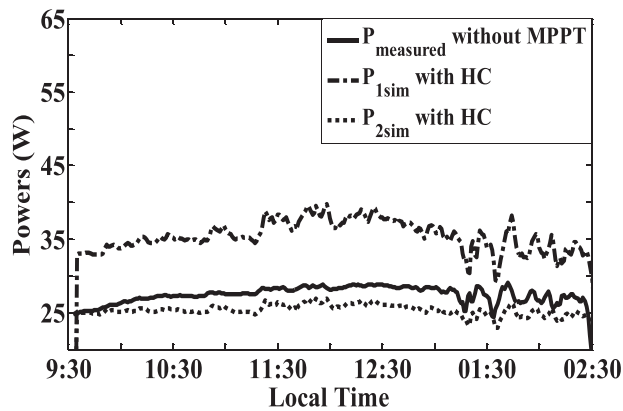


Fig. 12. Curves of output powers of the PV module using the Hill Climbing algorithm.

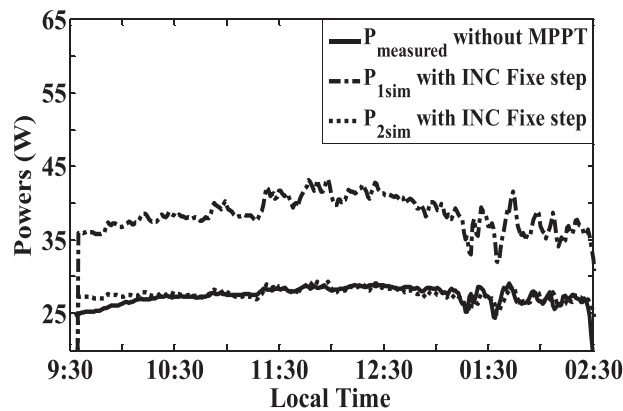


Fig. 13. Curves of output powers of the PV module using a fixed step INC algorithm.

addition, its profile is almost the same like the profile of the experimental curve measured without an MPPT module (solid line).

Obviously, it is well shown that with these two MPPT algorithms, the simulation curves of output power with the constant inputs intrinsic solar cell parameters are far from the expected output power, even if they are higher than the experimental curve. The P&O and the fixed step size INC algorithms have the same performance even if the output power is less than that of the variable step size INC. This low performance is certainly due to the difficult choice of

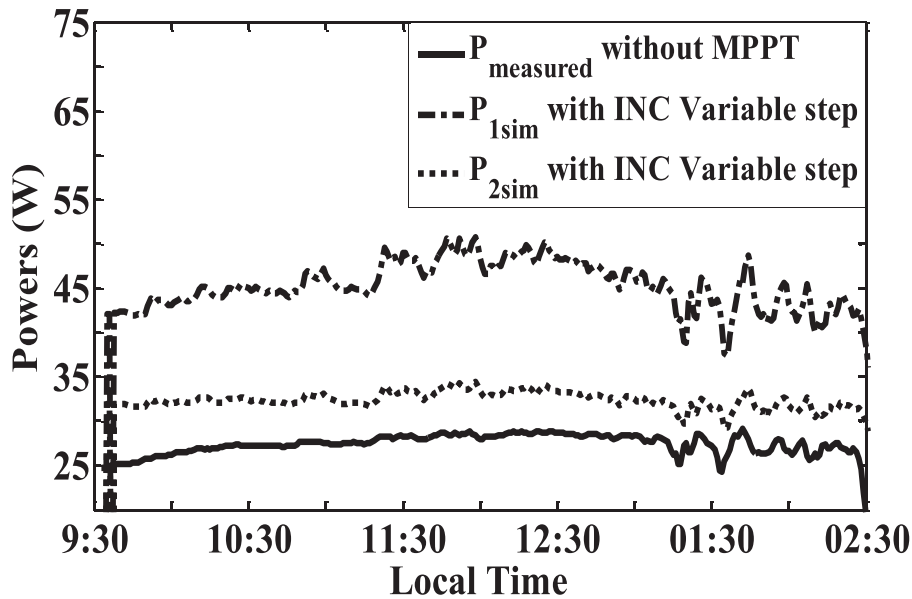


Fig. 14. Curves of output powers of the PV module using a variable step INC algorithm.

Table 3

Comparison of the daily production of energy of the crystalline silicon photovoltaic module for different MPPT algorithms.

Photovoltaic parameters	$R_S = 2.1 \Omega$, $n = 1.2$ and I_s (Dandoussou et al., 2015)				Variable PV parameters			
	(a)	(b)	(c)	(d)	(a)	(b)	(c)	(d)
Different MPPT algorithms								
Daily maximum power (W)	29.32	26.92	29.32	34.40	43.25	39.72	43.25	50.76
Daily average energy, E (Wh/day)	166.69	153.09	166.69	195.09	224.75	206.41	224.75	263.07

(a): P&O, (b): HC, (c): fixed step INC, (d): variable step INC.

the step size. In fact, if the step size is small, the algorithm is stable with a low convergence speed. If the step size is high, the algorithm is fast with instability around the MPP.

Table 3 presents the daily average energy produced by the photovoltaic module with the implemented MPPT algorithms. The average energy has been calculated by MATLAB® command for numerical integration: trapz (t,P), with t the time vector and P the power vector. Results show clearly that, with variable PV parameters, the daily average energy is higher compared to the daily average energy produced with constant PV parameters. The lowest energy is obtained with the HC algorithm whatever PV parameters are fixed or variable. The highest energy is obtained with the variable step INC algorithm whatever PV parameters are fixed or variable. However, the P&O and the fixed step INC algorithms have the same performance. These results show that the performance of an MPPT algorithm must be evaluated under normal operating conditions (NOC). In fact, theoretically, it has been proved that the HC algorithm has the best performance with an efficiency of 95–99% against 90–98% for the INC algorithm and 81–96% for the P&O algorithm (Kumar, 2013). This study shows that under NOC, the HC algorithm is the worst and the variable step INC algorithm is the best.

5. Conclusion

This work focused on the evaluation of the performance and the reliability of usual MPPT algorithms, taking into consideration the dependency of the intrinsic parameters of crystalline silicon photovoltaic modules to the variable weather conditions. These intrinsic parameters were extracted by fitting the I(V) characteristic to experimental points. In so doing, the responses of near to real Simulink® model of photovoltaic modules are superimposed with the experimental points. The obtained Simulink model of the PV module has been used to simulate with a good accuracy the MPPT

algorithms widely used i.e. Perturb and Observe (P&O), Incremental Conductance (INC), Hill-Climbing (HC). The simulation results show that the variable step size INC algorithm has the best performance and reliability than both HC and P&O algorithms in fast variable weather conditions. However, in order to reduce uncertainties in this work, the following items must be considered: the use of the various technologies of PV cells (monocrystalline, polycrystalline, amorphous, etc.), the influence of the other parameters like the shunt resistance and the band gap energy of the solar cell.

References

- Abdulkadir, M., Samosir, A.S., Yatim, A.H.M., Yusuf, S.T., 2013. A new approach of modelling, simulation of MPPT for photovoltaic system in Simulink model. *ARPN J. Eng. Appl. Sci.* 8 (July (7)).
- Alsadi, S., Alsayid, B., 2012. Maximum power point tracking simulation for photovoltaic systems using Perturb and Observe algorithm. *Int. J. Eng. Innov. Technol.* 2 (December (6)).
- Cho, Jae-Hoon, Hong, Won-Pyo, 2013. A variable step size incremental conductance MPPT of a photovoltaic system using DC–DC converter with direct control scheme. *J. Korean Inst. Illum. Electr. Install. Eng.* 27 (9), 74–82.
- Christopher, I.W., Ramesh, R., 2016. Comparative study of P&O and Inc MPPT algorithms. *Am. J. Eng. Res.* 2 (12), 402–408 (e-ISSN: 2320-0847, p-ISSN: 2320-0936) www.ajer.org.
- Dandoussou, A., Kamta, M., Bitjoka, L., Wira, P., Kuitché, A., 2015. Simulations based on experimental data of the behaviour of a monocrystalline silicon photovoltaic module. *J. Sol. Energy*, 9 (Article ID 169015).
- de Brito, M.A.G., Galotto, L., Sampaio, L.P., de Azevedo e Melo, G., Canesin, C.A., 2013. Evaluation of the main MPPT techniques for photovoltaic applications. *IEEE Trans. Ind. Electron.* 60 (March (3)).
- Durusu, Ali, Nakir, I., Ajder, A., Ayaz, R., Akca, H., Tanrioven, M., 2014a. Performance comparison of widely-used maximum power point tracker algorithms under real environmental conditions. *Adv. Electr. Comput. Eng.* 14 (3).
- Durusu, Ali, Nakir, I., Tanrioven, M., 2014b. Matlab/Stateflow based modeling of MPPT algorithms. *Proc. of the Intl. Conf. on Advances in Mechanical and Automation Engineering—MAE*, <http://dx.doi.org/10.15224/978-1-63248-022-4-41> (ISBN: 978-1-63248-022-4).
- Kumar, Ch.K., Dinesh, T., Kumar, S.G., 2013. Design and modelling of PV system and different MPPT algorithms. *Int. J. Eng. Trends Technol.* 4 (September (9)).
- Liu, F., Duan, S., Liu, F., Liu, B., Kang, Y., 2008. A variable step size INC MPPT method for PV systems. *IEEE Trans. Ind. Electron.* 55 (July (7)).
- Lokanadham, M., Vijaya Bhaskar, K., 2012. Incremental conductance based maximum power point tracking (MPPT) for photovoltaic system. *Int. J. Eng. Res. Appl.* 2 (March–April (2)), 1420–1424 (ISSN: 2248-9622) www.ijera.com.
- Rathod, G., Gorawar, M., Revankar, P.P., Tewari, P.G., 2014. Matlab based comparative studies on selected mppt algorithms for SPS system. *Int. J. Res. Eng. Technol.* 03 (July (07)) (eISSN: 2319-1163, pISSN: 2321-7308).
- Saravana Selvan, D., 2013. Modeling and simulation of incremental conductance MPPT algorithm for photovoltaic applications. *Int. J. Sci. Eng. Technol.* 2 (July (7)), 681–685 (ISSN: 2277-1581).
- Saxena, A.R., Gupta, S.M., 2014. Performance analysis of P&O and incremental conductance MPPT algorithms under rapidly changing weather conditions. *J. Electr. Syst.* 10 (3), 292–304.
- Tey, K.S., Mekhilef, S., 2014. Modified incremental conductance MPPT algorithm to mitigate inaccurate responses under fast-changing solar irradiation level. *Sol. Energy* 101, 333–342.